

# Variously substituted phenyl hepta cyclopentyl-polyhedral oligomeric silsesquioxane (ph,hcp-POSS)/polystyrene (PS) nanocomposites

## The influence of substituents on the thermal stability

Ignazio Blanco · Lorenzo Abate · Francesco Agatino Bottino

Italian Special Issue  
© Akadémiai Kiadó, Budapest, Hungary 2013

**Abstract** A comparative study concerning the thermal stability of polystyrene (PS) and six POSS/PS nanocomposites of general formula  $R_7R'(SiO_{1.5})_8/PS$  (where  $R =$  cyclopentyl and  $R' =$  phenyl, 4-methoxyphenyl, 4-tolyl, 3,5-xilyl, 4-fluorophenyl, and 2,4-difluorophenyl) was carried out in both inert (flowing nitrogen) and oxidative (static air) atmospheres. Nanocomposites were prepared by in situ polymerization of styrene in the presence of 5 % w/w of POSS, but the actual filler concentration in the obtained nanocomposites, determined by  $^1H$  NMR spectroscopy, was in all cases slightly higher than that in the reactant mixtures. FTIR spectra of nanocomposites evidenced the presence of filler-polymer interactions. Inherent viscosity ( $\eta_{inh}$ ) determinations indicated that the average molar mass of polymer in methylated and fluorinated derivatives was lower than neat PS, and were in agreement with calorimetric glass transition temperature ( $T_g$ ) measurements. Degradations were performed into a thermobalance, in the scanning mode, at  $10\text{ }^\circ\text{C min}^{-1}$ , and the temperatures at 5 % mass loss ( $T_5\%$ ), of various nanocomposites were determined. The effects of various substituents of the POSS phenyl group on the thermal stability of nanocomposites were evaluated. The results were discussed and interpreted.

**Keywords** POSS · Polystyrene nanocomposites · Thermal degradation · Thermogravimetric analysis

## Introduction

Organic–inorganic hybrid materials play currently a key role in the production of high performance materials because they possess much better characteristics than constituents. In particular, the introduction of inorganic nanostructures into polymers (nanocomposites) leads generally to the improvement of physical [1], mechanical [2], barrier [1], and flammability [3] properties in comparison with virgin polymer. Owing to these reasons, they have attracted great interest and have driven chemists, materials scientists, engineers, and physicists to synthesize novel products and investigate their possible applications in various fields.

Carbon nanotubes, layered silicates, and other [4–10] are used to prepare organic–inorganic hybrid systems, but, in the last decade, polyhedral oligomeric silsesquioxanes (POSSs) have attracted the attention for the use as fillers in the production of polymer-based nanocomposites [11, 12].

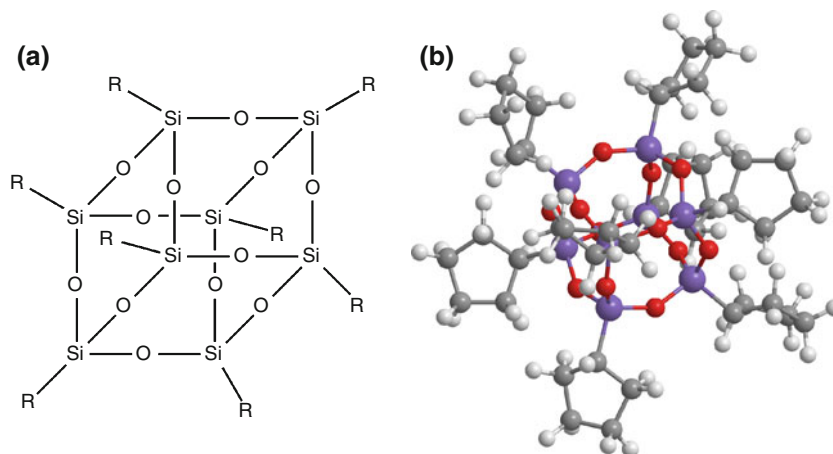
The POSS general formula is  $(R-SiO_{1.5})_n$ , where  $n = 8$ , the Si/O ratio is 2/3, while the organic R groups, which can be the same or different, are linked to a silicon–oxygen cage.

A typical POSS nanoparticle (Fig. 1) is thus formed by an inorganic  $Si_8O_{12}$  nanostructured cubic cage, surrounded by eight organic groups such as alkyl, aryl, or any of their derivatives, linked to the cage silicon atoms by covalent bonds [13].

The nature of these side groups largely affects both the solubility in conventional solvents and the compatibility with polymer matrices, then determining their capability to undergo nanometric dispersion into a host polymer, as well as the thermal stability of obtained nanocomposites. In particular, it has been reported in literature that POSSs having aliphatic groups bonded with silicon cage show the

I. Blanco (✉) · L. Abate · F. A. Bottino  
Department of Industrial Engineering, University of Catania,  
V.le A. Doria, 6, 95125 Catania, Italy  
e-mail: iblanco@dii.unict.it

**Fig. 1** Molecular structure of hcp-POSS **a** planar view, **b** three-dimensional view



improvement of solubility and compatibility, however, accompanied by the worsening of thermal properties, while the presence of aromatic groups acts in the opposite way [14].

Since some years we are interested in the study of polystyrene (PS)-based nanocomposites [15] to obtain products having better properties than virgin polymer, in particular higher thermal stability, which is important because these products can be subjected to high temperatures during processing or in service. A fine dispersion at molecular level of a POSS into polymer matrix is requested to obtain the best exploitation of its properties when used as filler for nanocomposites. Owing to this reason, we focused our attention on asymmetric  $R_7R'(SiO_{1.5})_8$ , owing to symmetric  $R_8(SiO_{1.5})_8$  leads generally to auto-aggregation phenomena of POSS molecules [16]. So, the opportune selection of R and R' groups can allow to obtain products where the chemical-physical filler-polymer interactions are prevalent on the POSS-POSS ones.

To this purpose, in the first part of our research, we synthesized and characterized some  $R_7R'(SiO_{1.5})_8$  POSSs, where R = cyclopentyl or isobutyl group and R' = unsubstituted  $C_6H_5-$  group or one of its mono- or di-substituted derivatives, where the presence of seven cycloaliphatic or aliphatic groups provides for a good compatibility with polymer [17].

Good thermal stability was found for both series of studied POSSs with better results for the cyclopentyl derivatives [18, 19].

Some preliminary investigations were thus carried out in order to verify if and at which concentration our POSSs give rise to nanocomposites with better thermal properties than neat PS [20–22].

Phenyl, hepta cyclopentyl-polyhedral oligomeric silsesquioxane/polystyrene (ph,hcp-POSS/PS) nanocomposites at various filler concentration were thus prepared by in situ polymerization of styrene in the presence of POSS, and their degradation was studied in both inert and oxidative atmospheres. The results obtained evidenced higher

thermal stability than neat polymer, which enhanced on increasing filler concentration up to 5 % POSS about [20], while it decreased as a consequence of a further filler percentage increment, probably owing to more POSS-POSS interactions [21].

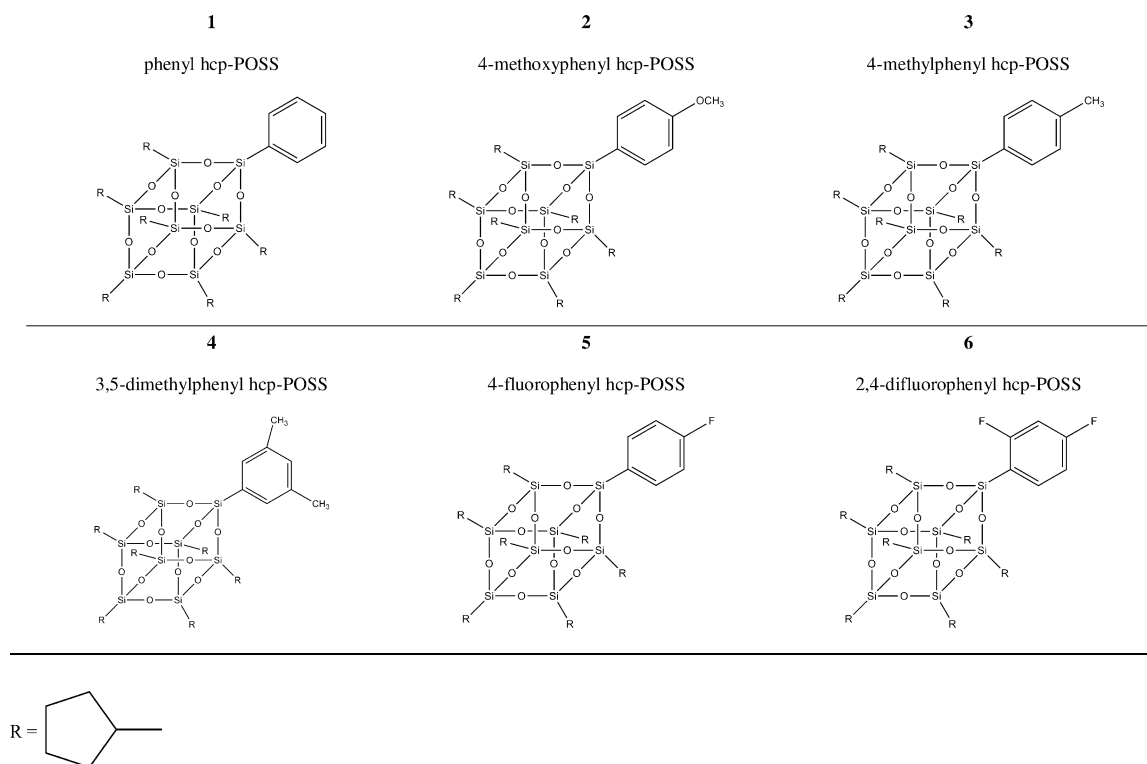
In order to have a more complete picture of the thermal behavior of the nanocomposites of our interest, in this work we carried out a comparative study of the thermal stability of the PS based nanocomposites having as fillers all the cyclopentyl POSSs previously studied [18]. The formulae of various POSSs are reported in Table 1. The samples to be analyzed were prepared from reactant mixtures at 5 % w/w POSS/PS, owing to this composition appeared to give rise, according to some of our preceding experiments [20], to nanocomposites showing most enhanced thermal stability than neat PS.

The characterization of PS and obtained nanocomposites was made by  $^1H$ NMR spectroscopy, to verify the actual filler content, and by differential scanning calorimetry (DSC) to determine glass transition temperature ( $T_g$ ). Also, inherent viscosity ( $\eta_{inh}$ ) measurements were carried out to check if the presence of various substituted POSSs affected the average molar mass of PS. Thermogravimetric (TG) and differential thermogravimetric (DTG) analysis, in both flowing nitrogen and static air atmosphere, were finally carried out to study the thermal behavior of our nanocomposites and to determine the temperature at 5 % mass loss ( $T_{5\%}$ ).

## Experimental

### Materials

Styrene (Aldrich Co.) was purified by passing it through an inhibitor removal column. 2,2-Azobis(isobutyronitrile) (AIBN) (98 % Aldrich Co.) was re-crystallized twice from dry ethanol at temperatures less than 40 °C and out of direct light. Toluene was stirred over calcium hydride for

**Table 1** Molecular structure of the various ph,hcp-POSS used for the synthesis of PS nanocomposites


24 h and distilled in a nitrogen atmosphere. Tetrahydrofuran (THF) was distilled over a Na–benzophenone mixture.

The preparation of variously substituted POSSs was first carried out. To this aim, phenyltrichlorosilane and *p*-tolyltrichlorosilane (Aldrich Co.) were used as received. 4-fluorophenyltrichlorosilane, 2,4-difluorophenyltrichlorosilane, 3,5-dimethylphenyltrichlorosilane, and 4-methoxyphenyltrichlorosilane were prepared from the appropriate Grignard reagent and SiCl<sub>4</sub> [23, 24]. Cyclopentyltrisilanol (*c* C<sub>5</sub>H<sub>9</sub>)<sub>7</sub>–Si<sub>7</sub>O<sub>9</sub> (OH)<sub>3</sub> was prepared according to the literature methods [25, 26]. Substituted POSSs were prepared by corner capping reaction of cyclopentyltrisilanol with the suitable aryltrichlorosilane in dry THF. The same procedure was used for all compounds. The details of preparation are reported in Ref. [18].

Nanocomposites were then prepared by in situ polymerization of 5 % w/w POSS/styrene mixtures in toluene. The details of free-radical polymerization procedure are described, as an example, for compound **2**.

Styrene monomer (3.80 g) and 4-methoxyphenyl hcp-POSS (0.20 g) were dissolved in 40 ml of toluene, and AIBN radical initiator (12 mg) was added; the mixture was frozen in a liquid nitrogen bath, degassed with a vacuum pump, and thawed. This operation was repeated three times and then the tube, sealed under vacuum, was heated at

70 °C for 24 h under stirring. The clear solution was poured into a large excess of methanol (600 ml), the precipitated nanocomposite was collected by filtration and dried under vacuum at 40 °C. The yield was 3.52 g (88 %).

The same polymerization procedure was used to prepare neat PS and compounds **1** (yield 85 %), **3** (yield 83 %), **4** (yield 80 %), **5** (yield 86 %), and **6** (yield 86 %).

#### <sup>1</sup>H NMR spectroscopy

<sup>1</sup>H NMR spectra were recorded using a Varian Unity Inova instrument (<sup>1</sup>H 500 MHz), using CDCl<sub>3</sub> as solvent and TMS as internal standard.

#### IR spectroscopy

Fourier transform infrared (FTIR) spectra were traced using a Perkin–Elmer Spectrum 100 spectrometer, using an universal ATR sampling accessory. Spectra were recorded at r.t. from 4000 to 600 cm<sup>−1</sup> with a resolution of 4.0 cm<sup>−1</sup>, directly on compounds, without any preliminary treatment.

#### Viscosity measurements

An Ubbelohde suspended-level viscosimeter and solutions of polymers in chloroform at the concentration of 1.0 g dL<sup>−1</sup>

and at temperature of  $25 \pm 0.1$  °C were used to measure inherent viscosities ( $\eta_{inh} = \ln \eta_r / C$ , where  $\eta_r$  = relative viscosity and  $C$  = polymer concentration).

### DSC measurements

A Mettler DSC 20 differential scanning calorimeter, coupled with a Mettler TC 10 A processor, was used for glass transition temperature ( $T_g$ ) determinations. The response of apparatus in enthalpy and temperature was calibrated according to the procedure suggested by the manufacturer [27]. To this purpose, two built-in programs of processor, which use the fusion of indium for the calibration of enthalpy and the melting points of three metals, indium, lead, and zinc, for that of temperature, were employed. The calibration of enthalpy, checked by the melting of fresh indium, showed an agreement within 0.25 % with the literature standard value of  $3.273 \text{ kJ mol}^{-1}$  [28, 29], while the accuracy of temperature, checked by several scans with fresh indium and tin, was in every case within 0.08 % in respect to literature data ( $156.6$  and  $231.9$  °C for indium and tin, respectively) [28, 29].

The calibrations were repeated every two weeks. Samples of about  $5.0 \times 10^{-3}$  g, held in sealed aluminum crucibles, a heating rate of  $10$  °C  $\text{min}^{-1}$  and flowing nitrogen ( $0.02 \text{ L min}^{-1}$ ) were used for measurements.

### TG analysis

The thermal degradations of the studied compounds were carried out into a Mettler TA 3000 thermobalance, coupled with the same Mettler TC 10 A processor as control and evaluation unit used for DSC measurements. The temperature of furnace was calibrated according to the procedure suggested by Mettler and reported in the user's manual of equipment [27]. This procedure, which is considered in literature the most precise [30], is based on the change of magnetic properties of three metal samples (Isatherm, Nickel and Trafoperm) at their Curie points ( $142.5$ ,  $357.0$ , and  $749.0$  °C, respectively). The temperature calibration was repeated every month.

Degradation experiments were carried out in dynamic heating conditions, from  $35$  up to  $700$  °C, in both flowing nitrogen ( $0.02 \text{ L min}^{-1}$ ), and a static air atmosphere, at the heating rate ( $\Phi$ ) of  $10$  °C  $\text{min}^{-1}$ . Samples of about  $5 \times 10^{-3}$  g, held in alumina open crucibles, were used and their masses were measured as a function of temperature and stored in the list of data of the appropriate built-in program of processor. The TG and DTG curves were immediately printed at the end of each experiment and the mass of sample at various temperatures were then transferred to a PC. These data were later used to plot the percentage of undegraded sample  $(1 - D)\%$  as a function of temperature, where

$D = (W_o - W)/W_o$ , and  $W_o$  and  $W$  were the masses at the starting point and during scanning.

### Results and discussion

Since previous experiments made by us [20, 22] showed that the filler percentages in nanocomposites obtained by in situ polymerization of styrene were slightly higher than those in reactant mixtures, the actual POSS contents in the nanocomposites prepared starting from mixtures at 5 % w/w POSS/PS were thus determined by  $^1\text{H}$  NMR spectroscopy. The filler percentages were calculated through the ratio of hydrogen atoms of filler and those of PS. All these values were quite in agreement with each other, but all were slightly higher than 5 % (Table 2).

The FTIR spectra of **1–6** compounds were thus carried out and compared with those of neat PS and corresponding POSSs. In all cases, the shift of the sharp band near  $1080 \text{ cm}^{-1}$ , present in the POSSs spectra and attributable to Si–O bonds, was observed in the nanocomposites spectra, thus indicating the presence of filler-polymer interactions. Since no substantial differences were found among various investigated POSS, for the sake of shortness we report here the spectra concerning the compound **6** only (Fig. 2), in which this band shifts from  $1078 \text{ cm}^{-1}$  (for the POSS) to  $1094 \text{ cm}^{-1}$  (for the nanocomposite).

In order to evaluate a possible dependence of nanocomposites thermal stability on polymer average molar mass, inherent viscosity determinations on studied compounds were thus performed and compared with that of neat PS. Only the  $\eta_{inh}$  values found for ph,hcp-POSS and 4-methoxy ph,hcp-POSS were the same than that of virgin polymer, thus indicating that, in these cases, the average molar mass of PS in nanocomposites was the same than that of neat polymer. The  $\eta_{inh}$  values found for the methyl- and dimethyl-derivatives were little lower than PS. Conversely, the inherent viscosities of F-nanocomposite and even more of diF-nanocomposite were much lower than that of neat polymer, thus suggesting a sharp decrease of PS average molar mass and then that fluorinated POSSs affect the polymerization process. The  $\eta_{inh}$  values of PS and studied nanocomposites are listed in Table 2.

The glass transition temperatures, which were also calorimetrically determined, exhibited a trend quite similar to that of inherent viscosity. Since  $\eta_{inh}$  and  $T_g$  are not only characteristic parameters of polymers but also their values are connected with the average molecular mass, the similar trend found for these two parameters indicates that the observed variations are driven by the same single factor, it means the average molar mass. Also, the  $T_g$  values are reported in Table 2.

The initial decomposition temperature ( $T_i$ ) is considered the key parameter to evaluate the resistance of polymer materials to thermal degradation [31, 32]. This parameter is obtained by the degradation TG curves as the intersection between the starting mass line and the maximum gradient tangent to the curve [33–35]. Since the  $T_i$  values so obtained largely depend on the slope of the descending piece of degradation TG curve, we preferred to determine temperature at 5 % mass loss which is a parameter correlated with initial decomposition temperature [36], but which is, in our opinion, more reliable to compare the thermal stability of various compounds because it is not depending on the kinetics of the most advanced degradation stages.

Degradation experiments were first carried out in inert atmosphere, in dynamic heating conditions, at the heating rate of  $10\text{ }^\circ\text{C min}^{-1}$ , which was selected because it is a medium scanning rate among those usually employed for

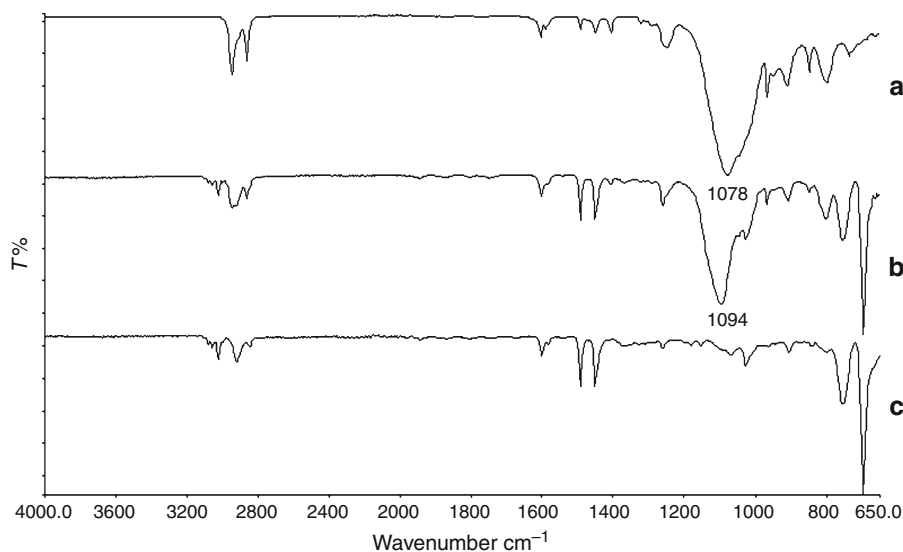
thermal degradations and is the same of that of our calorimetric  $T_g$  determinations. PS and all studied nanocomposites degraded in flowing nitrogen up to complete mass loss. The corresponding TG degradation curves are reported in Fig. 3, while the determined  $T_{5\%}$  values are listed in Table 2. Even though PS and its nanocomposites degraded in all cases up to complete mass loss, the TG curves exhibited a difference: PS and dimethyl-nanocomposite degraded completely in a single step, while other nanocomposites showed a first very sharp degradation stage, followed by a second one at low degradation rate in the last piece of TG curves, which is more evident for the compounds **1**, **5**, and **6** (Fig. 3). The behavior of our compounds in oxidative atmosphere (Fig. 4) was quite similar to that under nitrogen, and the corresponding  $T_{5\%}$  values are also listed in Table 2.

Also, we performed the FTIR spectra of the residues in air at  $430\text{ }^\circ\text{C}$ . This temperature, at which the samples mass is reduced to about the 10 % of the initial one, was selected because it is roughly the starting temperature of the low rate degradation stage. The FTIR spectra of the residues so obtained were compared with that of the residue at  $380\text{ }^\circ\text{C}$  (10 % about of initial sample mass) obtained from the degradation of neat PS and those of corresponding POSSs. The presence in the FTIR spectra of the residues of nanocomposites of the band at  $697\text{ cm}^{-1}$  and of some weak bands in the  $2900\text{--}3100\text{ cm}^{-1}$  range, which are present in PS spectrum, as well as of the band attributable to Si–O bonds, indicates that, during the second low rate degradation stage of nanocomposites, both polymer and filler are present at temperatures largely higher than that at which the complete decomposition of neat PS occurs (Fig. 4), thus indicating a further thermal stabilization of polymer. This finding confirms our previous results [20]. The FTIR spectra of the residues at  $430\text{ }^\circ\text{C}$  of compound **6** and the

**Table 2** POSS percentages, inherent viscosity ( $\eta_{\text{inh}}$ ), glass transition temperature ( $T_g$ ), temperature at 5 % mass loss ( $T_{5\%}$ ) of PS and various nanocomposites in static air atmosphere, and in flowing nitrogen

Compounds	Air static atmosphere				Nitrogen flow $T_{5\%}/\text{K}$
	POSS/%	$\eta_{\text{inh}}/\text{dL g}^{-1}$	$T_g/\text{K}$	$T_{5\%}/\text{K}$	
PS	–	0.17	372	511	573
<b>1</b>	5.9	0.17	372	558	606
<b>2</b>	6.8	0.17	373	569	588
<b>3</b>	6.4	0.16	369	539	581
<b>4</b>	6.6	0.16	369	509	565
<b>5</b>	6.8	0.15	370	556	581
<b>6</b>	6.9	0.12	368	550	570

**Fig. 2** FTIR spectra of 2,4-difluorophenyl hcp-POSS (a), sample **6** (b) and PS (c)



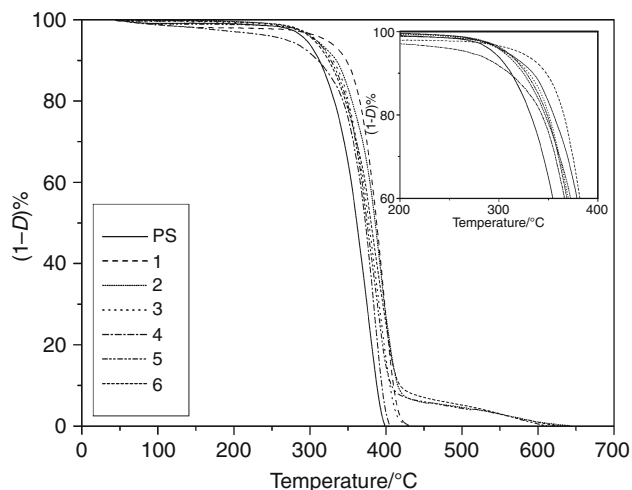


**Fig. 3** TG degradation curves at  $10\text{ }^{\circ}\text{C min}^{-1}$ , under nitrogen flow, of PS and various ph,hcp-POSS/PS nanocomposites

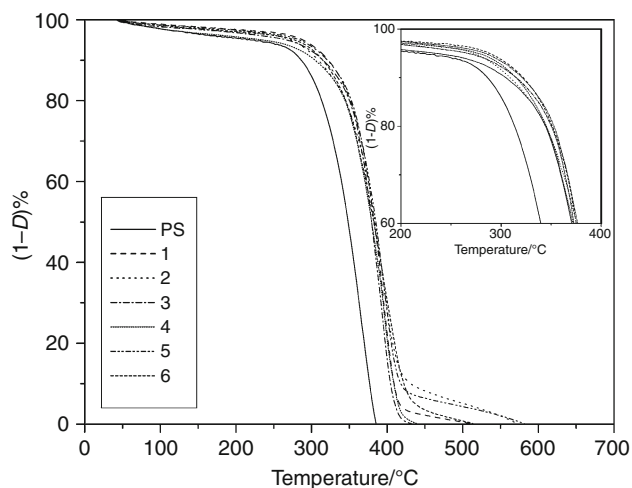
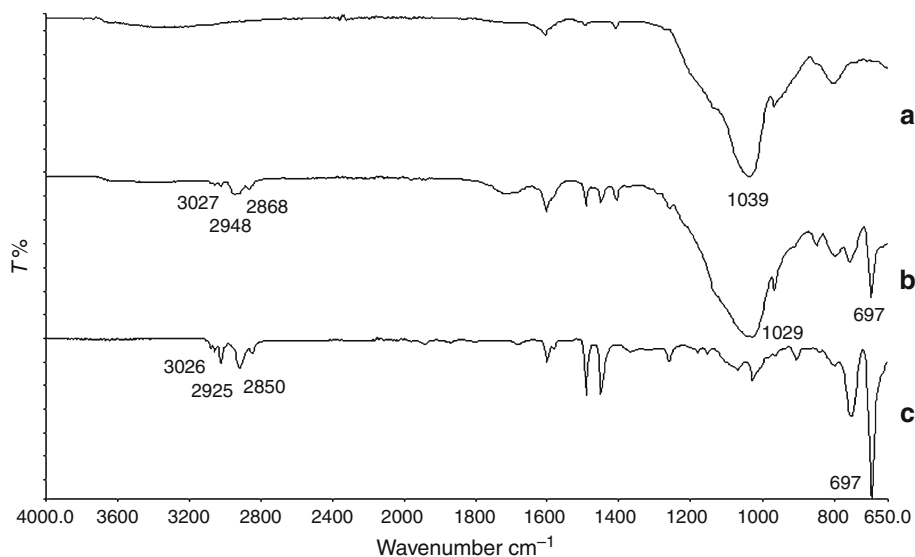


**Fig. 4** TG degradation curves at  $10\text{ }^{\circ}\text{C min}^{-1}$ , in static air atmosphere, of PS and various ph,hcp-POSS/PS nanocomposites

**Fig. 5** FTIR spectra of the residues of 2,4-difluorophenyl hcp-POSS (a), sample 6 (b), and PS (c) after thermal degradation in static air atmosphere



corresponding POSS are reported as an example in Fig. 5, together with that at  $380\text{ }^{\circ}\text{C}$  of PS.

The data in Table 2 suggest some considerations:

- the  $T_{5\%}$  values obtained for the unsubstituted 5% ph,hcp-POSS/PS nanocomposite were largely higher ( $33$  and  $47\text{ }^{\circ}\text{C}$  in flowing nitrogen and static air atmosphere, respectively) than those of neat PS, thus indicating a strongly enhanced resistance to the thermal degradation of nanocomposite in respect to virgin polymer;
- the introduction of a methoxy group on the POSS phenyl ring does not lead to any change of the inherent viscosity with respect to that of unsubstituted ph,hcp-POSS/PS. Conversely, the introduction of a methyl group and, more, of a fluorine atom, leads to the decrease of  $\eta_{inh}$  value, which is larger if two fluorine atoms are introduced. These results indicate that the presence of fluorinated POSSs reduces the PS polymerization degree and appear in agreement with  $T_g$  determinations owing to it is well known that glass transition temperature of polymers increases on increasing average molar mass [37];
- the unsubstituted ph,hcp-POSS/PS nanocomposite appears the most thermally stable in inert environment. The introduction of one substituent on the POSS phenyl group lowers the thermal stability of obtained nanocomposite independently on its electron-donor (as methyl or methoxy group) or electron-withdrawing (as fluorine atom) character, such as shown by the decrease in  $T_{5\%}$  values, which however is still higher than that of neat PS;
- the introduction on the POSS phenyl group of a second substituent, identical to the first one, leads to a further  $T_{5\%}$  decrease, but, in this case, up to lower values than that of virgin polymer;



- the  $T_5\%$  values obtained in oxidative atmosphere were lower than those under nitrogen, but the  $T_5\%$  increments in respect to neat PS were higher. The overall picture of the results in static air atmosphere substantially confirms that under nitrogen, apart from the methoxy derivative for which higher resistance to thermal degradation than unsubstituted ph,hcp-POSS/PS nanocomposite was found.

## Conclusions

The results over reported indicate that the unsubstituted ph,hcp-POSS is a good filler for producing PS nanocomposites with an optimum aromatic/aliphatic groups ratio, which insures a good compatibility of filler with polymer and, in the same time, high thermal stability of nanocomposite obtained. The introduction of aliphatic substituents on the POSS phenyl group seems to reduce the resistance to thermal degradation of nanocomposites, which appears depending of the number of substituents groups. The lowering of PS average molar mass when in situ polymerization is carried out in the presence of methylated or fluorinated POSS could also contribute to the decrease of thermal stability of corresponding PS nanocomposites.

## References

1. Gupta RK, Kennel E, Kim KJ, editors. Polymer nanocomposites handbook. Boca Raton: CRC Press Inc; 2010.
2. Pellice SA, Fasce DP, Williams RJJ. Properties of epoxy networks derived from the reaction of diglycidyl ether of bisphenol A with polyhedral oligomeric silsesquioxanes bearing OH-functionalized organic substituents. *J Polym Sci Part B*. 2003; 41(13):1451–61.
3. Philips SH, Gonzalez RI, Chaffee KP, Haddad TS, Hoflund GB, Hsiao BS, Fu BX. Remarkable AO resistance of POSS inorganic/organic polymer. In: Loud S, editor. Bridging the centuries with SAMPE's materials and processes technology. 45th International SAMPE symposium and exhibition. Society for the Advancement of Material and Process Engineering (SAMPE), Covina, California. 2000;45:1921–31.
4. Yu SL, Zuo XT, Bao RL, Xu X, Wang J, Xu J. Effect of SiO<sub>2</sub> nanoparticle addition on the characteristics of a new organic-inorganic hybrid membrane. *Polymer*. 2009;50:553–9.
5. Chrissafis K, Paraskevopoulos KM, Tsiaoussis I, Bikiaris D. Comparative study of the effect of different nanoparticles on the mechanical properties, permeability, and thermal degradation mechanism of HDPE. *J Appl Polym Sci*. 2009;112:1606–18.
6. Avella M, Cosco S, Di Lorenzo ML, Di Pace E, Errico ME. Influence of CaCO<sub>3</sub> nanoparticles shape on thermal and crystallization behaviour of isotactic polypropylene based nanocomposites. *J Therm Anal Calorim*. 2005;80(1):131–6.
7. Jiao C, Chen X. Synergistic effects of zinc oxide with layered double hydroxides in EVA/LDH composites. *J Therm Anal Calorim*. 2009;98(3):813–8.
8. Ramezanzadeh B, Attar MM, Farzam M. Effect of ZnO nanoparticles on the thermal and mechanical properties of epoxy-based nanocomposite. *J Therm Anal Calorim*. 2011;103(2):731–9.
9. Viratyaporn W, Lehman RL. Effect of nanoparticles on the thermal stability of PMMA nanocomposites prepared by in situ bulk polymerization. *J Therm Anal Calorim*. 2011;103(1):267–73.
10. Hu S, Hu Y, Song L, Lu H. Effect of modified organic-inorganic hybrid materials on thermal properties of cotton fabrics. *J Therm Anal Calorim*. 2011;103(2):423–7.
11. Kannan RY, Salacinski HJ, Odlyha M, Butler PE, Seifalian AM. The degradative resistance of polyhedral oligomeric silsesquioxane nanocore integrated polyurethanes: an in vitro study. *Biomaterials*. 2006;27(9):1971–9.
12. Kannan RY, Salacinski HJ, Ghanavi J, Narula A, Odlyha M, Peirovi H, Butler PE, Seifalian AM. Silsesquioxane nanocomposites as tissue implants. *Plast Reconstr Surg*. 2007;119(6):1653–62.
13. Mather PT, Jeon HG, Haddad TS. Strain recovery in POSS hybrid thermoplastics. *Polym Prepr*. 2000;41(1):528–9.
14. Fina A, Tabuani D, Carniato F, Frache A, Boccaleri E, Camino G. Polyhedral oligomeric silsesquioxanes (POSS) thermal degradation. *Thermochim Acta*. 2006;440(1):36–42.
15. Abate L, Blanco I, Bottino FA, Di Pasquale G, Fabbri E, Orestano A, Pollicino A. Kinetic study of the thermal degradation of PS/MMT nanocomposites prepared with imidazolium surfactants. *J Therm Anal Calorim*. 2008;91(3):681–6.
16. Fina A, Monticelli O, Camino G. POSS-based hybrids by melt/reactive blending. *J Mater Chem*. 2010;20:9297–305.
17. Fina A, Tabuani D, Frache A, Boccaleri E, Camino G. In: Le Bras M, Wilkie C, Bourbigot S, editors. Fire retardancy of polymers: new applications of mineral fillers. Cambridge, UK: Royal Society of Chemistry; 2005. p. 202–20.
18. Blanco I, Abate L, Bottino FA, Bottino P, Chiacchio MA. Thermal degradation of differently substituted cyclopentyl polyhedral oligomeric silsesquioxane (CP-POSS) nanoparticles. *J Therm Anal Calorim*. 2012;107(3):1083–91.
19. Blanco I, Abate L, Bottino FA, Bottino P. Hepta isobutyl polyhedral oligomeric silsesquioxanes (hib-POSS): a thermal degradation study. *J Therm Anal Calorim*. 2012;108(2):807–15.
20. Blanco I, Abate L, Bottino FA, Bottino P. Thermal degradation of hepta cyclopentyl, mono phenyl-polyhedral oligomeric silsesquioxane (hcp-POSS)/polystyrene (PS) nanocomposites. *Polym Degrad Stab*. 2012;97(6):849–55.
21. Blanco I, Bottino FA, Bottino P. Influence of symmetry/asymmetry of the nanoparticles structure on the thermal stability of polyhedral oligomeric silsesquioxane/polystyrene nanocomposites. *Polym Compos*. 2012;33(11):1903–10.
22. Blanco I, Bottino FA. Thermal study on phenyl, hepta isobutyl-polyhedral oligomeric silsesquioxane/polystyrene nanocomposites. *Polym Compos*. 2013;34(2):225–32.
23. Rosenberg SD, Walburn JJ, Ramsden HE. Preparation of some arylchlorosilanes with arylmagnesium chlorides. *J Org Chem*. 1957;22(12):1606–7.
24. Breed LW, Haggerty WJ Jr. Aryl and alkylchlorodialkoxysilanes. *J Org Chem*. 1960;25(1):126–8.
25. Feher FJ, Newman DA. Enhanced silylation reactivity of a model for silica surfaces. *J Am Chem Soc*. 1990;112(5):1931–6.
26. Feher FJ, Budzichowski TA, Blanski RL, Weller KJ, Ziller JW. Facile syntheses of new incompletely condensed polyhedral oligosilsesquioxanes: [(c-C<sub>5</sub>H<sub>9</sub>)<sub>7</sub>Si<sub>7</sub>O<sub>9</sub>(OH)<sub>3</sub>], [(c-C<sub>7</sub>H<sub>13</sub>)<sub>7</sub>Si<sub>7</sub>O<sub>9</sub>(OH)<sub>3</sub>], and [(c-C<sub>7</sub>H<sub>13</sub>)<sub>6</sub>Si<sub>6</sub>O<sub>7</sub>(OH)<sub>4</sub>]. *Organometallics*. 1991;10(7):2526–8.
27. User's manual TA 3000 System. Greifensee: Mettler Instr., AG, 1984.
28. Della Gatta G, Richardson MJ, Sarge SM, Stølen S. Standards, calibration, and guidelines in microcalorimetry. Part 2. Calibration standards for differential scanning calorimetry (IUPAC Technical Report). *Pure Appl Chem*. 2006;78(7):1455–76.

29. Abate L, Badea E, Blanco I, Della Gatta G. Heat capacities and enthalpies of solid–solid transitions and fusion of a series of eleven primary alkylamides by differential scanning calorimetry. *J Chem Eng Data*. 2008;53:959–65.
30. Csaba N. Handbook of thermal analysis and calorimetry. In: Gallagher Patrick K, Brown Michael E, editors. Principles and practice, vol. 1. Amsterdam: Elsevier; 1998.
31. Blanco I, Oliveri L, Cicala G, Recca A. Effects of novel reactive toughening agent on thermal stability of epoxy resin. *J Therm Anal Calorim*. 2012;108:685–93.
32. Blanco I, Siracusa V. Kinetic study of the thermal and thermo-oxidative degradations of polylactide-modified films for food packaging. *J Therm Anal Calorim*. doi:10.1007/s10973-012-2535-8.
33. Abate L, Blanco I, Cicala G, La Spina R, Restuccia CL. Thermal and rheological behaviour of some random aromatic polyethersulfone/polyetherethersulfone copolymers. *Polym Degrad Stab*. 2006;91(4):924–30.
34. Abate L, Blanco I, Cicala G, Recca A, Restuccia CL. Thermal and rheological behaviours of some random aromatic amino-ended polyethersulfone/polyetherethersulfone copolymers. *Polym Degrad Stab*. 2006;91(12):3230–6.
35. Abate L, Blanco I, Cicala G, Recca G, Scamporrino A. The influence of chain ends on the thermal and rheological properties of some 40/60 PES/PEES copolymers. *Polym Eng Sci*. 2009; 49(8):1477–83.
36. Abate L, Blanco I, Cicala G, Mamo A, Recca G, Scamporrino A. The influence of chain rigidity on the thermal properties of some novel random copolyethersulfones. *Polym Degrad Stab*. 2010; 95:798–802.
37. Chartoff RP. Thermoplastic Polymers. In: Turi A, editor. Thermal characterization of polymeric materials. 2nd ed. San Diego: Academic Press; 1997.